Tertiary-Structure Relaxation in Hemoglobin: A Transient Raman Study

Thomas W. Scott and Joel M. Friedman*

Contribution from AT&T Bell Laboratories, Murray Hill, New Jersey 07974.
Received November 26, 1982

Abstract: Tertiary relaxation in photodissociated hemoglobins has been monitored by using time-resolved resonance Raman scattering. It is observed that the submicrosecond tertiary-structure relaxation which precedes the switch in quaternary structure is sensitive to factors influencing R state stability. At pH 7 and lower, substantial relaxation involving the iron–proximal histidine linkage occurs over the time scale of geminate recombination. Because the structural parameter associated with the variation in this linkage has been implicated in the protein modulation of ligand binding, this result supports the idea of a dynamic barrier which increases on the time scale of geminate recombination. On the basis of these findings a model is presented which accounts for solution-dependent variations in ligand reactivity within a given quaternary structure.

There is considerable evidence that the two-state model is a good first-order description of Hb reactivity.[1,2] X-ray crystallographic studies have revealed two distinct quaternary structures for Hb.[1,3] The equilibrium between these two protein configurations is such that for the ligand-free (Fe^{+2}) or deoxy Hb, the T-state structure is favored, whereas for the ligand-saturated or ligated (oxy, carboxy, nitroxy) Hb, the R-state structure is favored. Many of the features of cooperative ligand binding in Hb are accounted for by assuming a saturation-dependent equilibrium between the low-affinity T and the high-affinity R structures. This description does not readily explain the observation that ligand binding can be varied by solution conditions that do not necessarily result in a quaternary switch.[4] Similarly there are species-specific differences as well that must be accounted for. Despite the fact that Hb has been extensively studied, several important mechanistic questions remain unanswered. They include the following: How does the overall quaternary structure regulate the localized ligand-binding process, how do the localized events at the oxygen-binding site bring about the large-scale structural changes associated with the quaternary structure, and how does solution-dependent or species-specific regulation of ligand affinity occur within a given quaternary structure. In this paper we describe a time-resolved resonance Raman scattering study of Hb, the results of which bear directly upon these questions.

The four oxygen-binding sites in Hb are four iron porphyrins or hemes. Each of the four polypeptide subunits (2α and 2β chains) comprising the Hb molecule contains one heme. Since the identical heme occurs both in the different animal species specific Hb's as well as in the two quaternary structures, variations in oxygen-binding properties must originate from differences in the protein matrix surrounding the heme binding site. The X-ray studies[3] reveal that in going from the ligand-free T state to the CO-saturated R state there is a large configurational change at the $\alpha_1\beta_2$ subunit interface. The two protein structures resulting from these two observed interfacial geometries are the two accessible quaternary structures for Hb. In the X-ray study[3] it was also observed that the protein structure about the heme within each subunit (tertiary structure) changes in switching from the deoxy T to the carboxy R state of Hb. From the X-ray study it is not possible to determine to what extent these tertiary structure differences originate from a pure R–T-induced change or from a ligation-induced difference. Furthermore, it is not readily discernable from these studies which of the differences in the tertiary structure are indeed perturbing the oxygen-binding site in a functional sense. It is therefore desirable to systematically probe the binding site, i.e., the heme, in a manner that reveals what is changing as a function of both state of ligation and quaternary state as well as which structural features correlate with ligand-binding properties. Since the binding of a ligand significantly perturbs the electronic and nuclear structure of the iron porphyrin, the anticipated subtle protein-induced effects upon the heme are not likely to be observed in a comparison of a deoxy and a ligated hemoglobin. Instead we require the hemes in all the comparisons to be in the identical electronic state. This requirement is accomplished by comparing R- and T-state varieties of both equilibrium deoxy forms of hemoglobin and transient deoxy species derived from photodissociated ligated hemoglobins. It has been shown that photodissociation and subsequent electronic relaxation to a ground-state deoxy (high spin-Fe^{+2}) heme occurs within 5 ps,[5-8] whereas appreciable or detectable protein relaxation does not appear to occur until at least many tens of ns subsequent to photodissociation.[9,10] Consequently, the transient species occurring within 10 ns of photolysis typically consist of deoxy hemes surrounded by a protein matrix that has the tertiary structure associated with the fully ligated parent species. Therefore, by spectroscopically comparing both R- and T-state varieties of deoxy and transient deoxy hemoglobins it should be possible to separate out the induced changes in the tertiary structure influencing the heme-associated degrees of freedom that originate from either ligation or change in the quaternary structure. By following both the relaxation of the structural features and any concomitant change in reactivity subsequent to photodissociation, one can hope to begin understanding the as yet undetermined coupling both between tertiary and quaternary structure as well as between structure and function.

Transient absorption studies have resulted in very effective measurements of the kinetics associated with the relaxation of the photoinduced ligand-free transient species of hemoglobin. On the microsecond time scale such studies[11] have revealed the rates of quaternary structure change subsequent to photolyzing R-state ligated Hb's. Similar absorption studies[10,12] as well as transient Raman study[9,13] in the nanosecond regime have revealed relaxation

(1) Perutz, M. F. *Proc. R. Soc. London, Ser. B* **1980**, *208*, 135–62.
(2) Shulman, R. G.; Hopfield, J. J.; Ogawa, S. *Q. Rev. Biophys.* **1975**, *8*, 325–420.
(3) Baldwin, J. M.; Chothea, C. *J. Mol. Biol.* **1979**, *129*, 175–201.
(4) DeYong, A.; Pennelly, R. P.; Jan Wilson, A. L.; Noble, R. W. *J. Biol. Chem.* **1976**, *251*, 6692. Kwiatowski, L. D.; Noble, R. W. *J. Biol. Chem.* **1982**, *257*, 8891–8895.
(5) Noe, L. J.; Eisert, W. G.; Rentzepis, P. M. *Proc. Natl. Acad. Sci. U.S.A.* **1978**, *75*, 573–577. Reynolds, A. H.; Rand, S. D.; Rentzepis, P. M. *Proc. Natl. Acad. Sci. U.S.A.* **1981**, *78*, 2292–2296.
(6) Greene, B. I.; Hochstrasser, R. M.; Weisman, R. B.; Eaton, W. A. *Proc. Natl. Acad. Sci. U.S.A.* **1978**, *75*, 5255. Chernoff, D. A.; Hochstrasser, R. M.; Steele, A. W. *Proc. Natl. Acad. Sci. U.S.A.* **1980**, *77*, 5606.
(7) Hutchinson, J. A.; Traylor, T. G.; Noe, L. J. J. *J. Am. Chem. Soc.* **1982**, *104*, 3321.
(8) Martin, J. L.; Migus, A.; Poyart, C.; LeCarpentier, T.; Astier, R.; Antosetti, A. *Proc. Natl. Acad. Sci. U.S.A.* **1983**, *80*, 173.
(9) Lyons, K. B.; Friedman, J. M. In "Hemoglobin and Oxygen Binding"; Ho, C., Ed.; Elsevier: New York, 1982, pp 333–338.
(10) Lindqvist, L.; Mohsni, El; Tfibel, F.; Alpert, B. *Nature (London)* **1980**, *28*, 729.
(11) Sawicki, C.; Gibson, Q. H. *J. Biol. Chem.* **1976**, *251*, 1533.
(12) Hofrichter, J.; Sommer, J. H.; Henry, E. R.; Eaton, W. A. *Proc. Natl. Acad. Sci. U.S.A.* **1983**, *80*, 2235.

0002-7863/84/1506-5677$01.50/0

dynamics ascribable to changes in the tertiary structure occurring prior to the R–T switch. Because the intrinsically broad absorption spectra of these molecules contain little structural information, it is not feasible to extract from these transient absorption studies information about what specifically is changing with time. Even a clear distinction between tertiary and quaternary relaxation is not unambiguous when using the porphyrin absorption as a probe. Alternatively the resonance Raman spectra of the heme is well characterized with respect to numerous porphyrin-associated degrees of freedom.[14,15] In addition the frequencies of several Raman bands originating from both stable and transient deoxy forms of Hb have been characterized with respect to features of the tertiary structure that are responsive to the quaternary structure and/or the state of ligation immediately (nanoseconds) prior to the excitation pulse.[13,16-18] The frequencies of some of these protein-sensitive Raman bands have been shown to correlate with ligand reactivity.[13] Amino acid sequence, pH, and temperature are known to alter ligand reactivity within a given quaternary state. To explore the structural basis for these and related effects within a given quaternary state we have used the transient Raman spectrum to probe the relaxation properties of specific Raman modes. In this study we determine the extent to which both the solution conditions such as pH and the animal source affect specific contributions to the tertiary relaxation within a given quaternary state. In addition, by using transient Raman spectroscopy we also generate instantaneous (10 ns) snapshots of the tertiary structure of nominally ligated Hb's as a function of temperature. And, as a means of demonstrating the potential efect of structural relaxation upon ligand reactivity, the nanosecond geminate recombination and microsecond bimolecular ligand rebinding are also monitored as a function of solution conditions for O_2HbA.

Experimental Procedure

Transient Raman spectra of Hb samples in aqueous solution were recorded on an apparatus previously described.[13] The spectra were generated with the 10-Hz output of a Lambda Physics excimer pumped dye laser (2002) which produces ~1-mJ pulses of ~10-ns duration and tuned to ~4350 Å (stilbene 2). For the single-pulse experiments, each pulse first photolyzed the sample and then generated the Raman spectrum of the transient within 10 ns. In the time-delay pulse-probe experiments, the initial photolyzing pulse (10 ns), consisting of the 4050-Å output of the nitrogen laser pumped dye laser, and the probe pulse (4350 Å) were electronically delayed with respect to each other. A pinhole apparatus ensured that the two pulses overlapped at the sample. The first pulse, which was partially defocussed, was larger in diameter than the probe pulse. To minimize the effect of geminate recombination upon the structural relaxation, some of the pulse-probe experiments were done at 35 °C. Under these conditions there is little recombination on the submicrosecond time scale for CO.

The geminate and bimolecular rebinding curves were generated by photolyzing an O_2HbA sample (10 °C, 1 atm of O_2) with the UV output of a nitrogen laser. The fraction of sites remaining deligated subsequent to photolysis was probed by monitoring the ratio of the deoxy (~1355 cm^{-1}) to the oxy (~1375 cm^{-1}) component of the ν_4 Raman band as previously described.[19] The Raman spectrum of the transient population was generated by using the excimer pumped dye laser (4400 Å). Because of a background fluorescence generated by the UV excitation pulse, accurate data points within 30 ns of the photolysis pulse were difficult to obtain.

Blood samples from the loggerhead sea turtle (*Caretta caretta*), green sea turtle (*Chelonia mydas*), and the Kemp's ridley sea turtle (*Lepidochelys kempi*) were taken from the jugular venous sinus of healthy subadult (~5 years old) individuals. Blood samples from the fresh-water turtles and the elephant trunk snake (*Achrochordus javanicus*) were obtained by direct cardiac puncture of live healthy specimens. Mutant human hemoglobins as well as hemoglobins from bluefin tuna (*Thunnis thynnis*), swordfish, carp, and cat were obtained as gifts from other laboratories. The hemoglobins were typically purified, asseyed, and stored in liquid N_2 as the carboxy derivative. Oxy derivatives were generated either by photolyzing the cooled (1 °C) carboxy form under a stream of oxygen or by oxygenating the freshly purified reduced hemoglobins. Stock concentrated solutions of purified Hb (either oxy or carboxy) were routinely passed through Sephadex G-25 columns before being diluted with appropriate buffers to heme concentrations of between 80 and 200 μM.

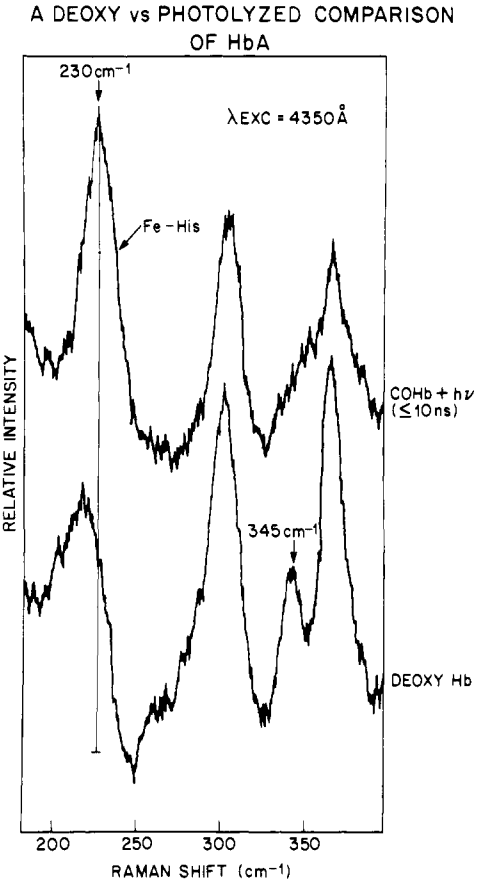

Figure 1. A comparison of the low-frequency Raman spectra of the equilibrium form of deoxy HbA and the transient deoxy HbA generated within 10 ns of photodissociating COHbA.

Results

Figure 1 shows the low-frequency resonance Raman spectrum of deoxy HbA and photolyzed COHbA. The deoxy HbA is an equilibrium species which is stabilized in the T-state quaternary configuration. COHbA is an R-state species. The species generated within 10 ns of photodissociating the COHbA contains deoxy hemes surrounded by an unstable protein structure. We designate the deoxy transient species occurring within a time t of photolysis as deoxy Hb*(t) which at least initially has the quaternary and tertiary structure of the parent R-state ligated protein (Hb*(t = 0) = Hb(R*l*)). The tertiary structure about a given heme for Hb*(t = 0) is therefore designated as Hb(R*l*). The tertiary structures of the deoxy R, ligated T, and deoxy T states are designated as Hb(Rd), Hb(T*l*), and Hb(Td), respectively. For each of these structures the heme can be either ligated or deoxy. Comparison of the two spectra in Figure 1 reveals differences which are attributable to the effects of the two different protein structures upon the deoxy hemes. We focus upon two specific Raman bands seen in the figure. One of them is the low-frequency (215–230 cm^{-1}) mode which has been assigned as the iron-proximal histidine (Fe–His) stretching motion.[20,21] The other is the low-intensity peak observed at ~345 cm^{-1} for the deoxy HbA sample. Examination of Figure 1 reveals that in going from deoxy HbA to deoxy Hb*(10 ns), the Fe–His frequency

(13) Friedman, J. M.; Scott, T. W.; Stepnoski, R. A.; Ikeda-Saito, M.; Yonetani, T. *J. Biol. Chem.* **1983**, *258*, 10564.
(14) Spiro, T. G.; *Isr. J. Chem.* **1981**, *21*, 81.
(15) Asher, S. A. *Methods Enzymol.* **1981**, *76*, 371–413.
(16) Friedman, J. M.; Rousseau, D. L.; Ondrias, M. R. *Annu. Rev. Phys. Chem.* **1982**, *33*, 471.
(17) Rousseau, D. L.; Ondrias, M. R. *Annu. Rev. Biophys. Bioeng.* **1983**, *12*, 357–80.
(18) Friedman, J. M. "Time Resolved Vibrational Spectroscopy"; G. Atkinson, G. Ed.; Academic Press: New York, 1983; pp 307–315.
(19) Friedman, J. M.; Lyons, K. B. *Nature (London)* **1980**, *284*, 570.

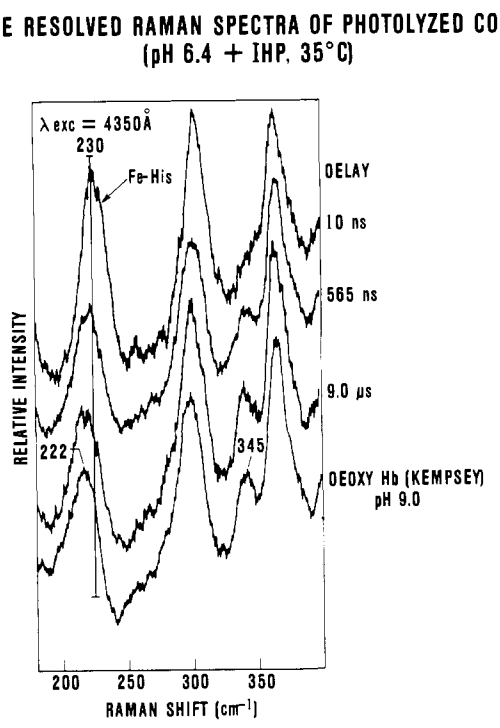

Figure 2. The time evolution of the low-frequency Raman spectrum of the deoxy photoproduct Hb* generated from COHbA. For comparison purposes an equilibrium R-state deoxy Hb spectrum derived from Hb-(Kempsey) at pH 9 is also shown in the figure. Photolysis of the COHbA was accomplished with a 10-ns excitation pulse (4050 Å, ~1 mJ). The Raman spectra were generated with an electronically delayed second 10-ns pulse (4350 Å, ~5 mJ). The sample was maintained at 35 °C in order to reduce geminate recombination.

(ν_{Fe-His}) increases from ~215 to 230 cm^{-1} while the 345-cm^{-1} peak shifts to higher frequency becoming a shoulder on the 360-cm^{-1} peak. The intense 360-cm^{-1} peak appears to be frequency invariant for all stable and transient hemoglobin samples examined.

In Figure 2 is shown the low-frequency Raman spectrum of deoxy Hb*(t) at several time delays subsequent to photolysis. The bottom spectrum is from deoxy Hb(Kempsey) at high pH. In contrast to HbA this mutant human hemoglobin is stabilized in the R structure at high pH even when ligand free. It can be seen that after a few microseconds subsequent to photolysis the spectrum of deoxy Hb*(t) is very nearly identical with that of the deoxy Hb(Kempsey). A comparison with the spectrum of deoxy HbA indicates that whereas the 345-cm^{-1} band is fully developed at 9 μs the Fe–His frequency has yet to relax to the equilibrium value of ~215 cm^{-1}. Subsequent relaxation of ν_{Fe-His} from the deoxy R-state value toward the equilibrium T-state value (~215 cm^{-1}) is shown in Figures 3 and 4 for COHbA and COHb (*Chelonia mydas*), respectively. COHb from the green sea turtle (*Chelonia mydas*) was chosen for the comparison because the photolyzed transient exhibits an anomolously low value for ν_{Fe-His}—only a few cm^{-1} higher than for the deoxy form (see Figure 11). It can be seen that after ~10 μs a broad low-frequency contribution begins to appear. This broad component is characteristic of the deoxy T-state species as can be inferred from the last spectrum in each figure.

A summary of the 35 °C relaxation measurements on the Fe–His mode is shown in Figure 5. The top portion of the figure shows the variation in the rate and extent of relaxation for the Fe–His frequency for human adult (HbA) deoxy Hb*(t) at different pH values. The bottom portion contains the comparable time evolution data for deoxy Hb*(t)'s derived from the loggerhead sea turtle (*Caretta caretta*) and the bluefin tuna (*Thunnus thynnis*). At pH 9 and 7 this low-affinity sea turtle hemoglobin is still cooperative,[22-24] whereas the tuna hemoglobin at pH 5.8

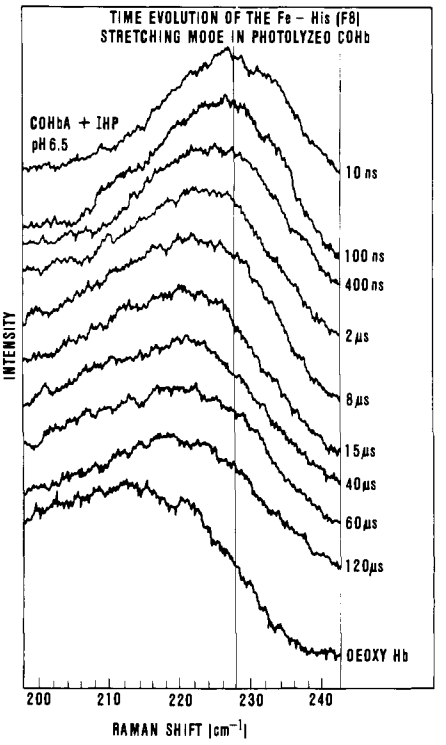

Figure 3. Time evolution of the Raman band associated with ν_{Fe-His} of deoxy Hb* (human) at pH 6.5 at 25 °C. The corresponding Raman band from the equilibrium deoxy HbA is shown at the bottom of the figure.

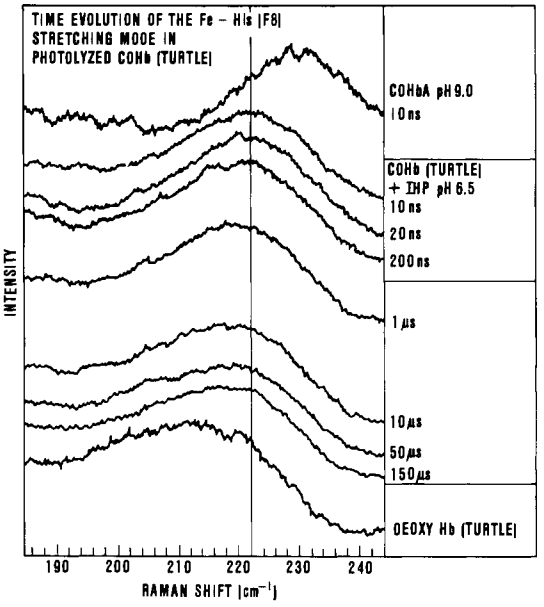

Figure 4. Time evolution of the Raman band associated with the ν_{Fe-His} of deoxy Hb* (green sea turtle, *Chelonia mydas*) at pH 6.5. Also shown in the figure are the corresponding Raman bands from photolyzed COHbA at 10 ns (top) and from the equilibrium deoxy form of Hb (*Chelonia mydas*) shown at the bottom.

remains a T-state species both with and without ligands.[25] Because of the low intensity, the corresponding plot for the 345-cm^{-1} peak was not attempted. Nevertheless, the relaxation of the 345-cm^{-1} peak closely follows the general trend observed for the Fe–His shown in Figure 5. Lowering the pH increases the re-

(20) Hori, H.; Kitagawa, T. *J. Am. Chem. Soc.* **1980**, *102*, 3608–13.
(21) Kitagawa, T.; Nagai, K.; Tsubaki, M. *FEBS Lett.* **1979**, *104*, 376.
(22) Lapennas, G. N.; Lutz, P. *Respir. Physiol.* **1982**, *48*, 59–74. Lutz, P.; Lapennas, G. N. *Respir. Physiol.* **1982**, *48*, 75–87. Lutz, P. In "A Comparison to Animal Physiology"; Cambridge University Press: New York, 1982; pp 65–72.
(23) Louro, S. R.; Bemski, *FEBS Lett.* **1982**, *14*, 293–6.
(24) Friedman, J. M.; Simon, S. R.; Scott, T. W. *Copeia*, in press.
(25) Morris, R. J.; Gibson, Q. H. *J. Biol. Chem.* **1982**, *257*, 4869–74.

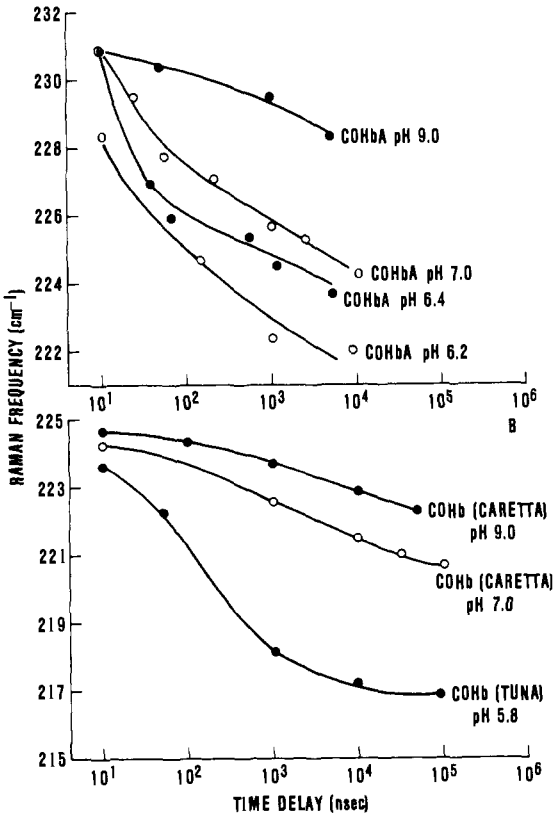

Figure 5. Time evolution of ν_{Fe-His} in Hb* as a function of solution conditions and animal source. The top portion of the figure shows the response to pH for photolyzed COHbA. The low-pH samples were also in the presence of ~1 mM IHP. The bottom part of the figure shows the time evolution of ν_{Fe-His} in samples derived from the loggerhead sea turtle (*Caretta caretta*) and the bluefin tuna (*Thunnis thynnis*).

laxation rates of both peaks. It appears that although the relaxation rates are similar they do not follow each other exactly. An accurate assessment of this statement is difficult because of both the weakness of the 345-cm^{-1} peak and the difficulty in assigning a peak position at intermediate points between the 345-cm^{-1} peak and the shoulder at 355 cm^{-1}. Furthermore, whereas in the low-pH HbA samples the relaxation of the 345-cm^{-1} peak is virtually complete at delays of a few microseconds, the Fe–His frequency is still far from the equilibrium value of ~215 cm^{-1} associated with T-state deoxy HbA as seen in Figures 3 and 4.

In Figure 6 is shown the O_2 rebinding curve for photolyzed O_2HbA at pH 8.3 (Tris 0.1 M) and at pH 7.0 + 3 mM IHP. It can be seen that both the rate and extent of rebinding are affected by the solution conditions. Both the geminate process occurring on the ~50–100-ns time scale and the slower bimolecular process are similarly affected. From a separate experiment it appears that the 10-ns averaged yield of photolysis is the same for these two samples.

Figures 7 and 8 display several transient Raman spectra of photolyzed O_2 HbA at 10 ns as a function of different temperatures. These spectra show the average heme pocket configuration associated with each of the specified conditions. It can be seen in Figure 7 that at pH 6.4 the 4 °C spectrum has no distinct 354-cm^{-1} peak whereas at the higher temperature even in the presence of 1.5 atm of O_2 the 345-cm^{-1} peak is prominent. In going from low to high temperature, ν_{Fe-His} shifts from 226 to 222 cm^{-1}. The high-temperature spectra resembles the deoxy R-state spectrum of deoxy Hb(Kempsey) shown on the bottom of the figure. Not shown in the figure are the corresponding COHbA spectra. Using CO as a ligand results in a series of nearly temperature invariant spectra all resembling the 4 °C O_2HbA spectrum in Figure 7. In Figure 8 is shown the temperature dependence of the 10-ns spectra of photolyzed O_2HbA at pH 9. Under atmospheric conditions the spectrum, which does not change

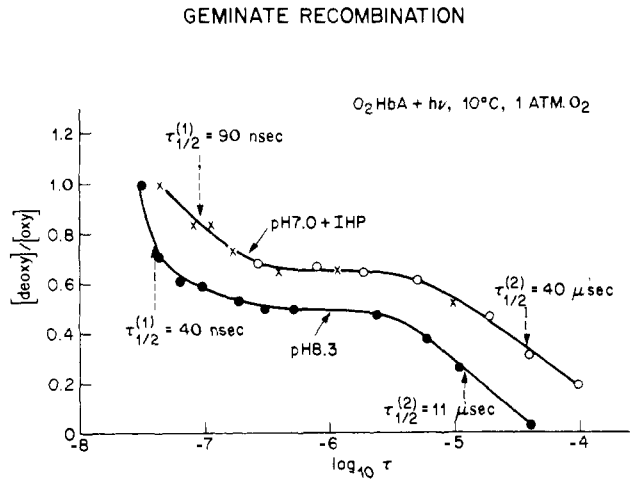

Figure 6. Ligand rebinding in photolyzed O_2Hb. The change in the deoxy-to-ligated ratio was determined from the ratio of the 1355–1375-cm^{-1} Raman bands (ν_4).

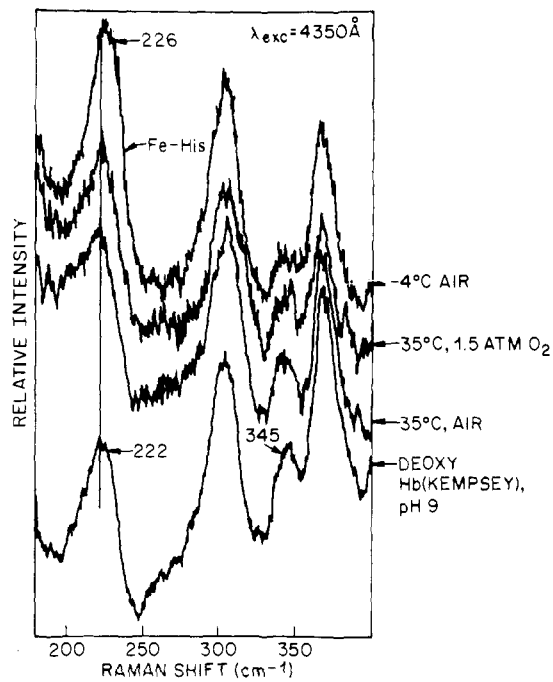

Figure 7. The effect of temperature upon the transient (10 ns) Raman spectrum of deoxy Hb* (human) at pH 6.4 + IHP. The deoxy photoproduct is derived from the O_2Hb. An equilibrium R-state deoxy species is shown at the bottom of the figure.

in going from 5 to 35 °C, has a ν_{Fe-His} of 230 cm^{-1} and no distinct 345-cm^{-1} peak. If, however, the sample chamber is flushed briefly with N_2 (resulting in a significantly reduced O_2 concentration) the high-temperature spectra reveal the appearance of a 345-cm^{-1} peak and at 40 °C ν_{Fe-His} has shifted to ~225 cm^{-1}. COHbA under all these conditions continues to resemble the 5 °C spectrum. In contrast to HbA at pH 9, the lower affinity Hb (*Chelonia mydas*) exhibits a much more prominent change with temperature as seen in Figure 9. It can be seen that in going from 20 to 35 °C, the N_2-flushed oxy sample displays a sizable shift of ν_{Fe-His} and an increase in the 345-cm^{-1} peak. The spectrum in the presence of CO (at 37 °C) is also shown. A distinctly different type of temperature response is seen in Figure 10. Figure 10 shows the effect of temperature of COHb from the bluefin tuna. It can be seen that in contrast to the other hemoglobins, ν_{Fe-His} increases with increasing temperature. The 345-cm^{-1} peak remains insignificant at both temperatures.

Discussion

The Fe–His Stretching Mode. The frequency of the Fe–His mode (ν_{Fe-His}) in hemoglobin has been characterized with respect

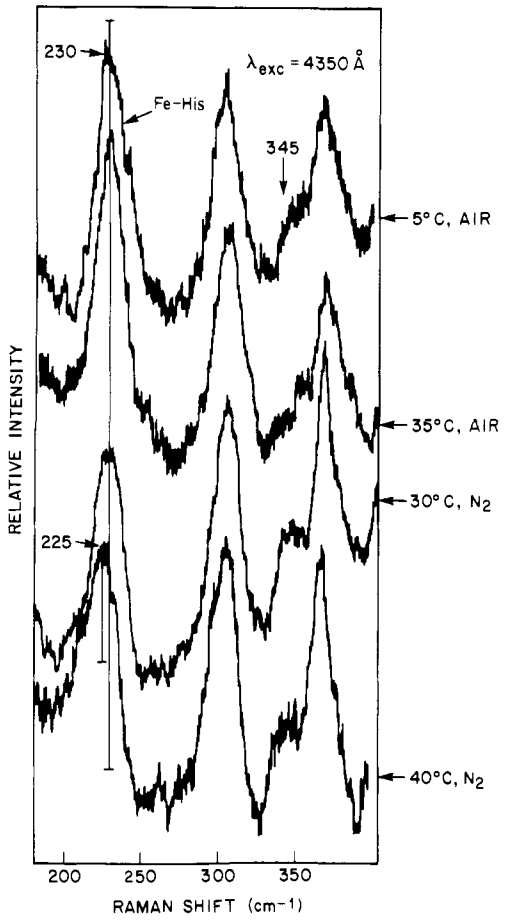

Figure 8. The effect of temperature upon the transient (10 ns) Raman spectrum of Hb* (human) at pH 9 The starting material was O_2HbA. The samples designated N_2 were flushed with N_2 after oxygenation.

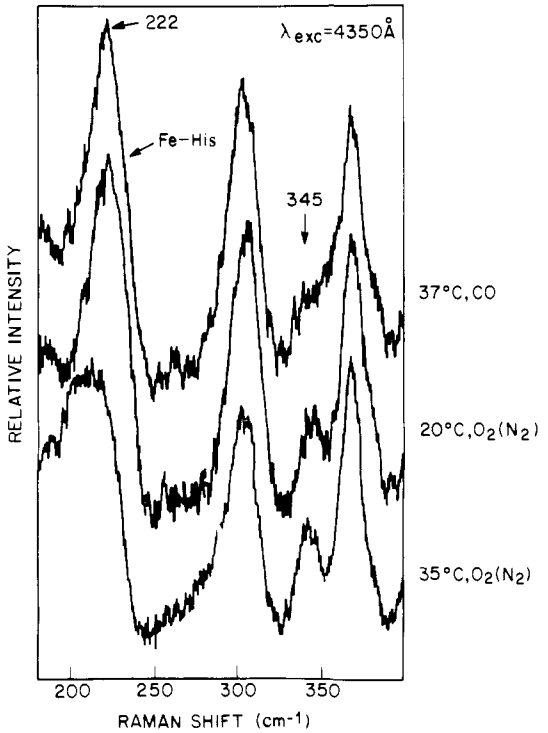

Figure 9. The effect of temperature upon the transient (10 ns) Raman spectrum of Hb* (*Chelonia mydas*; green sea turtle) derived from both oxy and carboxy samples at pH 9.

to tertiary structural rearrangements induced both by ligation and by quaternary structure changes. Studies on steady-state[17,26-28]

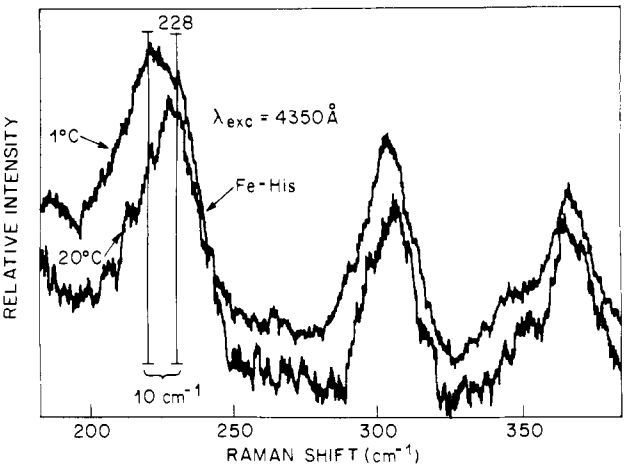

Figure 10. The effect of temperature upon the transient Raman spectrum of photolyzed COHb (tuna, *Thunnis thynnis*) at pH 7.0.

and transient forms[13,29,30] of deoxy hemoglobin have revealed that in going from the T state to the R state ν_{Fe-His} increases. In particular, the continuous wave Raman studies on stable T- and R-state deoxy hemoglobins show that in the T-state forms ν_{Fe-His} is typically 215 cm^{-1} whereas for the R-state species it is higher by several cm^{-1} (e.g., 222 cm^{-1} for deoxy Hb(Kempsey) at pH 9). Similar studies[28] on (Fe–Co) hybrid hemoglobins have revealed the distinct contribution of the α and β subunits to these frequencies. For deoxy HbA, ν_{Fe-His} for the β component is 218 cm^{-1} while a doublet is observed for the α subunit with frequencies of 202 and 212. In the R-state species they appear quite similar at 221 ± 2 cm^{-1} with the β subunit slightly higher.

Additional structural changes influencing the frequency of the Fe–His mode induced by ligation have been observed by using time-resolved Raman scattering[13,26,31-33] and continuous wave Raman[39,40] on liquid and frozen samples, respectively. The transient deoxy species observed within 10 ns of photolysis invariably have a higher frequency Fe–His mode than the corresponding equilibrium deoxy species within the same quaternary state. For example, deoxy HbA (deoxy (Hb(Td)) has a frequency of ~215 cm^{-1} while ~222 cm^{-1} is observed for deoxy Hb*(10 ns) = deoxy Hb(T*l*) derived from either COHb (Kansas) or NOHb(A) at low pH in the presence of IHP. Both of these samples are T-state species. Similarly for R-state Hb(Kempsey) (deoxy Hb(Rd)) the frequency is 222 cm^{-1} which increases to ~230 cm^{-1} for deoxy Hb*(10 ns) = deoxy Hb(R*l*) derived from COHbA, NOHbA, O_2HbA, COHb (Kempsey), and COHb (Kansas) all at high pH (8.5–9) and low ionic strength (≤0.1 M Cl^-). Consequently we have the following ordering with respect to the frequency of the Fe–His mode in deoxy Hb's: T-state deoxy Hb < T-state deoxy Hb*(10 ns) ≈ R-state deoxy Hb < R-state deoxy Hb*(10 ns) [Hb(Td) < Hb(T*l*) ≈ Hb(Rd) < Hb(R*l*)].

A summary of the variation in ν_{Fe-His} for deoxy Hb* (10 ns) as a function of both solution conditions and animal source is shown in Figure 11. The R–T arrow at the bottom of the figure indicates that those Hb's to the right of the marker are R-state species whereas those to the left are T-state species. Most of these

(26) Nagai, K.; Kitagawa, T.; Morimoto, H. *J. Mol. Biol.* **1980**, *136*, 271–89. Nagai, T. Kitagawa, *Proc. Natl. Acad. Sci. U.S.A.* **1980**, *77*, 2033–2037.
(27) Ondrias, M. R.; Rousseau, D. L.; Shelnutt, J. A.; Simon, S. R.; *Biochemistry* **1982**, *21*, 3428–3437.
(28) Ondrias, M. R.; Rousseau, D. L.; Kitagawa, T.; Ikeda-Saito, M.; Inubushi, T.; Yonetani, T. *J. Biol. Chem.* **1982**, *257*, 8766–70.
(29) Irwin, M. J.; Atkinson, G. H. *Nature* **1981**, *293*, 317.
(30) Stein, P.; Turner, J.; Spiro, T. G. *J. Phys. Chem.* **1982**, *86*, 168.
(31) Friedman, J. M.; Stepnoski, R. A.; Noble, R. W. *FEBS Lett.* **1982**, *146*, 278.
(32) Friedman, J. M.; Rousseau, D. L.; Ondrias, M. R.; Stepnoski, R. A. *Science* **1982**, *218*, 1244.
(33) Scott, T. W.; Friedman, J. M.;f Ikeda-Saito, M.; Yonetani, T. *FEBS Lett.* **1983**, *158*, 68–71.

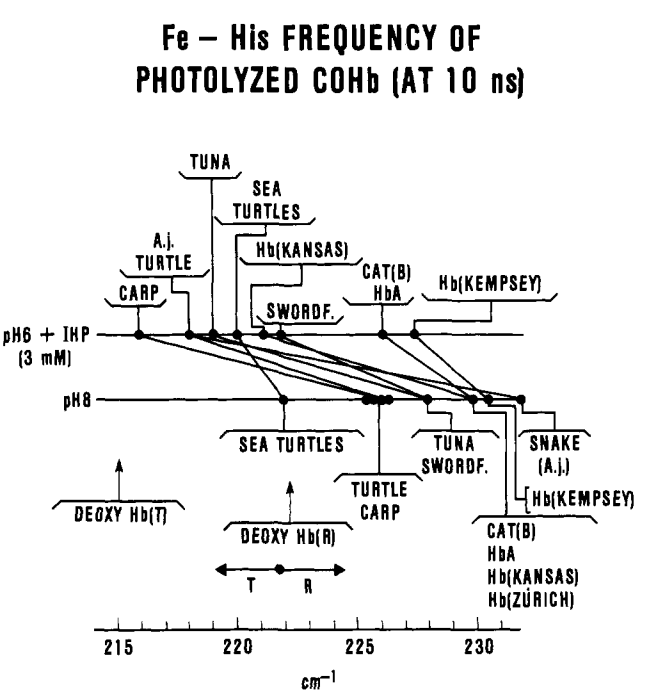

Figure 11. ν_{Fe-His} of Hb* at 10 ns a a function of pH and animal source. In all cases Hb* was derived from the carboxy form of the protein. Typical values of ν_{Fe-His} for equilibrium forms of the R- and T-state deoxy hemoglobins are also shown. The T–R arrows provide a rough indication of the quaternary structure of parent-ligated species of the Hb*'s shown in figure. The abbreviations shown in the figure stand for A.j. = *Acrochordus javanicus* (elephant trunk snake) and swordf = swordfish. Under the category of turtle are included five different fresh-water turtles while the catagory of sea turtle includes the green, leatherback, loggerhead, and Kemp's Ridley sea turtles.

quaternary state assignments are based upon independent measurements using a variety of techniques including kinetic, optical, NMR, and CD. Those assignments (sea turtles, turtles, and swordfish) not reported in the literature were established by CD and kinetic measurements (S. Simon, to be published). The two solution conditions used in the figure provide a means of determining the full dynamic range of the protein structure of the ligated Hb with respect to the iron–proximal histidine linkage. Representative values for deoxy R- and T-state hemoglobins are also indicated in the figure.

As with the stable deoxy forms, studies on hybrid transient hemoglobins have been useful in revealing subunit specific-frequency differences. It was observed[13,33] that for the R-state Hb*(10 ns) at high pH both α and β subunits have a frequency of $\sim$230 cm^{-1}. Below pH 6.8 in the presence of 3 mM IHP, $\alpha(FeCO)_2\beta(Co)_2$ appears to be predominantely a T-state species. The observed broad Fe–His Raman band at $\sim$217 cm^{-1} is characteristic of a mixed population of hemes some of which have the deoxy T and some the ligated T tertiary structures. Under these conditions ν_{Fe-His} for $\alpha(Co)_2\beta(FeCO)_2$ is $\sim$224 cm^{-1} which is indicative of a strained ligated R-state heme pocket (vis-â-vis 230 cm^{-1} at pH 9). COHbA under these same conditions displays a composite ν_{Fe-His} that is a few cm^{-1} higher than that for $\alpha(Co)_2\beta(FeCO)_2$ indicating that the pH plus IHP effect is essentially due to a change in the heme pocket of the β subunit. This conclusion is strongly supported by the observation[34] that it is primarily the ligand off rate of the β subunit and not the α subunit that is increased by IHP.

In both deoxy Hb[35] and deoxy Hb*[36] it has been observed that the porphyrin oxidation state marker band at $\sim$1355 cm^{-1} (also called ν_4 or band I) displays the same sensitivity to protein structure as ν_{Fe-His}. The frequency of this Raman band has been shown to be sensitive to the π-electron distribution of the porphyrin macrocycle.[37,38] Raman studies[35,36] have shown a progressive increase in electron density of the π*-porphyrin orbital in going from T-state deoxy Hb to T-state deoxy Hb*(10 ns) $\approx$ R-state deoxy Hb to R-state deoxy Hb*(10 ns). More recent studies on both steady-state[17,27] and transient species[26] have demonstrated that the frequencies of the Fe–His and this oxidation state marker band exhibit an inverse linear correlation. Such a correlation is consistent with the π density being modulated by changes in the iron–proximal histidine linkage.[1]

The 345-cm^{-1} Band. The assignment for the 345-cm^{-1} band is as yet uncertain. In contrast to the Fe–His mode, the 345-cm^{-1} band displays minimal sensitivity to the quaternary state.[18,39,40] In all R- and T-state deoxy hemoglobins examined (including those from lower vertebrates) this band appears as a distinct peak at $\sim$345 cm^{-1} (see Figure 1). In the corresponding spectra from a similar assortment of deoxy Hb*(10 ns)'s, (Hb(R*l*), and Hb(T*l*)) the band, now shifted to higher frequency, is seen only as a shoulder on the low-frequency side of the 360-cm^{-1} peak. These differences are observed both at ambient and cryogenic temperatures. However, in Hb(Zürich), a mutant human hemoglobin with a β-heme pocket that is substantially modified on the distal side, this shift from a distinct 345-cm^{-1} peak to a shoulder at $\sim$355 cm^{-1} is not nearly as evident despite an observed ν_{Fe-His} of 230 cm^{-1} for Hb(R*l*).[41] The conclusion from these studies is that there is an R–T-independent ligation-induced structural change at the heme in hemoglobin that is in some fashion dependent on the distal structure. The effects of this ligation-induced change persist in the Raman spectrum of deoxy Hb* for at least 10 ns subsequent to photolysis. Thus this portion of the Raman spectrum, when generated by nanosecond excitation, indicates the prior ligation history of a deoxy heme, i.e., whether the tertiary structure about the porphyrin has relaxed to a deoxy-like configurations or whether it still retains structural memory of an initially ligated state. Equipped with the above information about both the 345-cm^{-1} band and the Fe–His mode, we are now in a position to assess the structural implications of Figures 2–10.

Tertiary-Structure Relaxation: The Nature of Hb*. Microsecond transient absorption studies of deoxy Hb* have revealed a deoxy-like absorption spectrum that is shifted and broadened with respect to deoxy Hb.[42] Comparable submicrosecond studies show a similar but more exaggerated shift and broadening for deoxy Hb*($t \leq 10$ ns).[10,12] Transient Raman experiments discussed in this and in earlier papers not only bridge the ns gap but also shed considerable light on the nature of Hb*(t). In Figure 2 it can be seen that at 9 μs subsequent to photolysis, the frequency of the Fe–His of deoxy Hb* has relaxed to $\sim$222 cm^{-1}. This frequency is consistent with either an R-state deoxy structure (Hb(Rd)) or an unrelaxed photolyzed T-state species (Hb(T*l*)). The presence of a distinct 345-cm^{-1} peak indicates that the tertiary structure has relaxed to a deoxy configuration about the heme. It follows that the low-pH transient at $\sim$9 μs is the R-state deoxy HbA, a nonequilibrium species with respect to the quaternary structure. For deoxy Hb*(10 ns $< t <$ 1 μs), the higher frequencies for the Fe–His mode and the absence of a fully developed 345-cm^{-1} band indicates that the tertiary structure still retains features or "memory" of the ligated R-state parent species. Figure 5 shows that the relaxation of the ligation-associated contribution to the frequency of the Fe–His mode is a function of the stability of the R-state quaternary structure. Conditions which destabilize the R state such as lowering the pH and adding IHP cause an

(34) Ikeda-Saito, M.; Yonetani, T. *J. Mol. Biol.* **1980**, *138*, 845–858.
(35) Shelnutt, J. A.; Rousseau, D. L.; Friedman, J. M.; Simon, S. R. *Proc. Natl. Acad. Sci. U.S.A.* **1979**, *76*, 4409–13.
(36) Friedman, J. M.; Stepnoski, R. A.; Stavola, M.; Ondrias, M. R.; Cone, R. L. *Biochemistry* **1982**, *21*, 2022–2028.
(37) Spiro, T. G.; Burke, J. M. *J. Am. Chem. Soc.* **1976**, *98*, 5482–5489.
(38) Tsubaki, M.; Nagai, K.; Kitagawa, T. *Biochemistry* **1980**, *19*, 379–385.
(39) Ondrias, M. R.; Rousseau, D. L.; Simon, S. R. *J. Biol. Chem.* **1983**, *258*, 5638–5642.
(40) Ondrias, M. R.; Friedman, J. M.; Rousseau, D. L. *Science* **1983**, *220*, 615.
(41) Scott, T. W.; Friedman, J. M.; V. Macdonald, submitted for publication.
(42) Gibson, Q. H. *Biochem. J.* **1959**, *71*, 293.

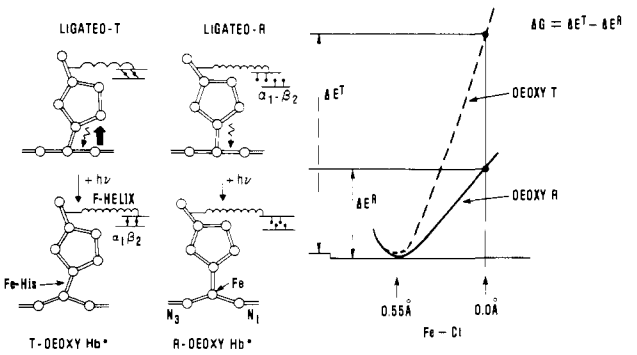

Figure 12. The effect of tilting the proximal histidine upon the energetics of ligand binding and the possible interplay between the histidine orientation and the α_1-β_2 interface.

increase in the relaxation of both the Fe–His mode and the 345-cm^{-1} peak. The observations that the Raman spectrum of Hb*(10 ns) is the same over a very large pH range, that at 10 ns the frequency of the Fe–His mode is at the high value limit while the 345-cm^{-1} peak is absent, and that the transient absorption spectrum for photolyzed COHbA does not evolve from several ps to several ns[6-8] subsequent to photolysis indicate that once the subpicosecond electronic relaxation to a deoxy heme has occurred,[8] deoxy Hb* reflects the tertiary structure of ligated R-state heme pocket until the pH-dependent ns relaxation beings.

The Relationship between Orientation of the Proximal Histidine and the Raman Spectrum. The tilt or cant of the proximal histidine within its own plane with respect to the heme plane is a structural parameter that has been associated with the variation in ν_{Fe-His}.[31,13,18] We now expose the implications of this association. This tilt affects the Fe–His bond by decreasing the separation between the imidazole carbon and the same side pyrrole nitrogen. A decrease in this distance increases the repulsive force between the imidazole and the heme which weakens the Fe–His bond causing a decrease in the frequency of the Fe–His stretching mode within the small tilt approximation. Thus for a fixed displacement of the iron, we associate a decrease in this Raman frequency with an increase in the histidine tilt. Since the frequencies observed in both steady-state and transient Raman studies indicate that, for comparisons of either the deoxy or transient deoxy species, the corresponding R-state hemoglobin has a less tilted geometry, it should be possible using X-ray crystallography to test this relationship by monitoring the histidine tilt in both R- and T-state deoxyhemoglobins as a function of ν_{Fe-His}. The tilt in the transient deoxy species can in principle be probed by pulse probe type experiments in which a crystal of a carboxy hemoglobin is probed structurally with pulsed X-rays both with and without a preceding optical photolysis pulse.

In the upper left side of Figure 12 we see a representation of the initial unphotolyzed R- and T-state ligated sample. On the basis of the X-ray studies,[3] we have the iron in plane. This histidine is shown to be upright for the R state and tilted for the T state. Upon photodissociating the ligated heme, the iron moves to an out-of-plane geometry within at most a few vibrational periods.[31] This conclusion is based upon both theoretical studies, which show that for a five-coordinate heme the very sizable repulsive forces between the imidazole carbons and the pyrrole nitrogens[43-45] are significantly reduced by the iron moving ~0.3 Å out of the plane,[45] and transient absorption results, which demonstrate that the subpicosecond kinetics for photodissociated hemes are indpendent of the protein matrix.[8] The above findings plus the observed constancy of the transient absorption spectrum from picoseconds to nanoseconds after photolysis[6] support the idea that deoxy Hb*(5 ps < t < 20 ns) contains a deoxy heme with a displaced iron. Aside from accommodating the motion of the iron the protein structure is virtually unrelaxed with respect to the ligated configuration. The frequency of the Fe–His stretching mode in the nanosecond spectra reflects this transiently frozen geometry of the deoxy Hb*. The difference in the frequency of the Fe–His mode between R- and T-state Hb*(10 ns)'s arises from tilt or other strain-induced variations in the distance between the imidazole carbon and the pyrrole nitrogen. An increase in the tilt results in a weakening of the Fe–His bond through an increase in the repulsive force between the carbon and the pyrrole nitrogen. As long as the iron is sufficiently displaced out of the heme plane the localized energy difference between the tilted and untilted geometry is small. However, the repulsive force increases substantially for the tilted configuration when the iron moves into the heme plane. This is shown schematically in Figure 12 where a decreasing iron-to-porphyrin center distance (Fe–Ct) results in a progressive divergence in the localized energy of the tilted (T) and less tilted (R) five-coordinate heme because of the repulsive forces discussed above. The figure indicates that it is energetically more costly to move the iron into the heme plane for the tilted species. Also shown in Figure 12 is a proposed interaction between the tilt and the configuration at the α_1-β_2 interface. When the iron is out of the heme plane, the histidine heme repulsive forces are reduced and the T-state configuration of the α_1-β_2 interface determines the overall histidine geometry. However, in the ligated species the energetics are now determined by the strong repulsive forces arising from the histidine tilt which may be transmitted to the α_1-β_2 interface via the F helix. A switch to the R-state interface reduces the tilt and relieves the tilt-induced strain for the ligated heme. In this working model, ligation- and deligation-induced protein dynamics result from an imbalance in the forces generated by the iron coordinate associated repulsive force and the quaternary structure dependent α_1-β_2 interface. When the iron is out of plane the interface dominates whereas when the iron is in plane the repulsive force is dominant.

Figure 12 depicts the ligated T-state species as having the same tilt as the deoxy T-state photolyzed transient; however, the accuracy of this representation depends upon the rigidity of other parts of the coupled heme–protein system. For example, if the T- and R-state structures are totally rigid the deoxy T and photolyzed ligated T at 10 ns should exhibit the same spectra as should the corresponding pair for the R state. Instead distinct and persistent (over many 10's of ns) differences are observed indicating that within each quaternary state there is a well-defined reorganization of the tertiary structure. The pattern of shifts observed for ν_{Fe-His} indicates that the structures having the highest value for ν_{Fe-His} are those that most stabilize the ligated heme. This pattern is also consistent with a description in which the localized strain induced by ligand binding to a deoxy T-state heme (with a ν_{Fe-His} of 215 cm^{-1}) is partially delocalized from the histidine heme unit via a limited or restricted tertiary reorganization. It is limited in that ν_{Fe-His} of the photolyzed ligated T-state transient still reflects potential strain when the iron is in plane. Within the tilt description the ν_{Fe-His} of photolyzed ligated T-state hemoglobin indicates only a partial reduction of the tilt. The question remains as to whether the strain associated with moving the iron in plane for this tilted configuration remains localized at the heme–histidine interface or is propogated to a weaker link in the coupled system—perhaps straining the bonds at the T-state α_2-β_2 interface as implied in Figure 12. If after the ligation-induced tertiary reorganization, the T-state structure is totally rigid and the spectrum of the ligated heme should reflect the still tilted and hence highly localized strained configuration. Raman experiments[17] on T- and R-state ligated hemoglobins reveal no substantial differences in the iron–ligand bond for the CO complexes indicating that for those cases the histidine is probably forced upright and the strain shuttled to another portion of the proteins. That the 10-ns transients do reflect differences at the heme indicates that as the iron moves out of the plane this delocalized strain is rapidly shuttled back to the now accomodating heme–histidine interface. In contrast to CO, there is evidence

(43) Warshel, A. *Proc. Natl. Acad. U.S.A.* **197**, *74*, 1789–1793.
(44) Gelin, B. R.; Karplus, M. *Proc. Natl. Acad. Sci. U.S.A.* **1977**, *74*, 801–805.
(45) Olafson, B. D.; Goddard, W. A., III *Proc. Natl. Acad. Sci. U.S.A.* **1979**, *74*, 1315–1319. Goddard, W. A.; Olafson, B. D. In "Biochemical and Chemical Aspects of Oxygen"; Caughy, W., Ed.; Academic Press: New York, 1979; pp 87–123.

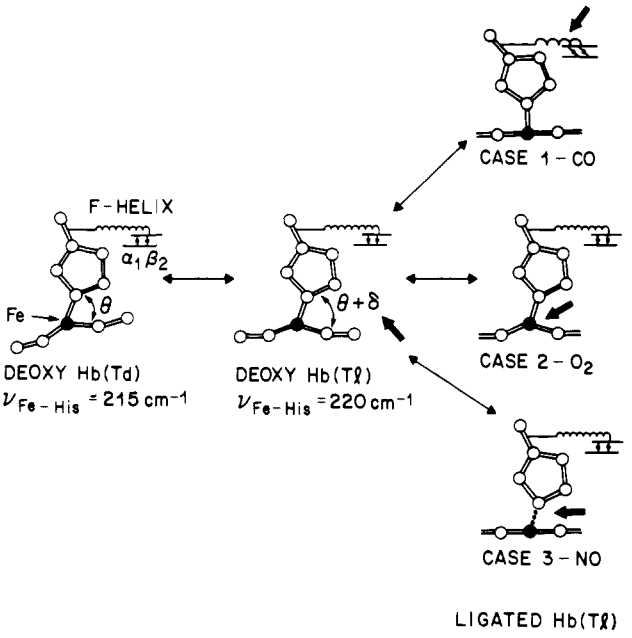

Figure 13. Possible pathways for the ligation-induced delocalization of strain generated from the titled proximal histidine configuration of T-state hemoglobin. Starting on the left is the equilibrium T-state deoxy heme configuration, Hb(Td), which because of the low value of ν_{Fe-His} (215 cm^{-1}) has the greatest tilt (designated by θ, the tilt angle). Upon ligand binding there is a tertiary reorganization, here arbitrarily represented by a tilting of the heme plane, which increases the tilt angle by δ and is reflected in the increased value of ν_{Fe-His} observed for the deoxy T-state photoproducts at 10 ns independent of ligand. Thus part of the strain energy that would be localized in the heme–histidine linkage upon ligation-induced movement of the iron into the heme plance for the Hb(Td) configuration is taken up by the tertiary reorganization to Hb(T*l*). This reorganization partially relieves the localized strain. Because the maximum room temperature value of ν_{Fe-His} appears to be ~230 cm^{-1}, the $\theta + \delta$ configuration of Hb(T*l*) is still considered to be tilted vis-à-vis Hb(R*l*). Within the Hb(T*l*) tertiary structure the fate of the residual tilt induced strain energy for the ligated heme appears to be ligand specific. In the case of CO, strain energy appears well removed from the heme[17] possibly residing at the α_1–β_2 interface as shown in case 1. For O_2, the X-ray data[54] suggest that the iron remains out of the plane in which case the iron–ligand–heme unit takes up the strain. For NO the strain is reduced in the α subunits by a rupture or a profound modification of the NO-weakened Fe–His linkage. The heavy arrows indicate the possible repositories for the strain energy which, it must be emphasized, is in all these cases assumed to originate from the repulsive forces between the imidazole carbon and the same side pyrrolnitrogen (see Figure 12).

from an X-ray crystallographic study[54] of partially oxygenated T-state hemoglobin that for O_2 the weak link is the Fe–O_2–heme unit. The data reveal that the oxygenated iron of the α chain remains substantially displaced proximally to the heme plane. Yet another pattern of strain redistribution is observed when NO is the ligand. Allegedly the Fe–proximal histidine bond is ruptured

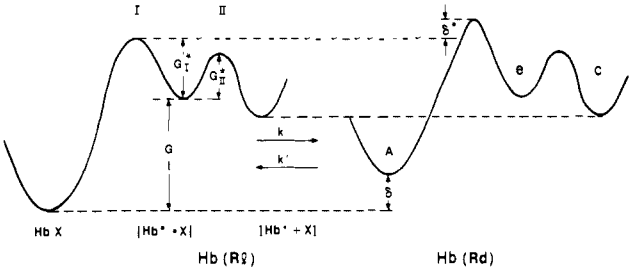

Figure 14. The reaction coordinate diagrams describing geminate rebinding in the ligated R-state (Hb(R*l*)) and the deoxy R-state (Hb(Rd)) tertiary structures. Potential well A corresponds to the ligated heme, HbX, while B and C refer to deoxy hemes with the ligand either in the heme pocket, [Hb* · X], or in the bulk protein, [Hb* + X], respectively. It is assumed that such potential surfaces can be assigned to a given tertiary structure of the protein. The designation Hb* indicates a deoxy heme modulated by the nonequilibrium protein structure associated with a tertiary structure other than the equilibrium deoxy species. Hb* would of course be different for Hb(R*l*) and Hb(Rd). Upon ligand dissociation it is assumed that the system is adiabatically switched from the ligated (A) well to the deoxy (B) well. The only associated structural changes are those that accommodate and accompany the very rapid relaxation of the heme to a nonplanar high-spin species. Rebinding from B and C gives rise to the subnanosecond and the ~100-ns geminate recombination processes, respectively.

or severly perturbed in the α chain of T-state NO hemoglobin.[55] This alteration is believed to be caused by a general weaking of the iron–histidine bond due to the electronic properties of NO.[56] The rupture of this weakened bond in the highly tilted T state α subunits is then the result of that bond being the weakest link in the ligand–heme–histidine–protein unit. That ν_{Fe-His} in Hb* is an indication of the potential strain in the ligated species is found in another NO-based experiment (J. M. Friedman and M. R. Ondrias, unpublished results). It was observed that whereas NOHbA at pH 8.5 shows the anticipated Raman spectrum[55c] associated with a population of hexacoordinate hemes, NOHb(Chelonia mydas) at the same pH exhibited a Raman spectrum reflecting a small but readily detectable population of pentacoordinate hemes. Under these conditions both NOHb's are R-state species; however, the associated ν_{Fe-His} for Chelonia is ~222/cm^{-1} (see Figure 11)—only slightly higher than typical T-state values. This low value indicates that even within the R structure the heme histidine unit remains a source of strain energy in this low-affinity hemoglobin.[22] HbA under these conditions has a ν_{Fe-His} of 230 cm^{-1}. Upon lowering the pH and adding IHP both NOHb's exhibit the same T-state hexa–penta mixture as well as typical T-state Hb* values for ν_{Fe-His}. A pictorial summary of some of the above possible ligand-dependent repositories for the strain energy originating from the heme–histidine repulsive interaction is shown in Figure 13.

The consequence of Figure 12 and the above discussion is that it is now possible to discuss the contribution of a specific structural parameter, i.e., the heme–histidine tilt, to the mechanisms of protein control of ligand binding. For a given hemoglobin, a specific frequency of the Fe–His mode is associated with a specific configuration of the heme–histidine linkage. If we assume that the bond formation between the ligand and the iron is fast compared to changes in the protein conformation about the heme then with each Fe–His frequency we can associate a potential surface that describes the ligand-binding dynamics for a ligand that is in the vicinity of a binding site. In order to get an estimate for the general shape of an appropriate potential surface one must consider what is known about the dynamics of ligand binding within the heme pocket. The most relevant studies are those that focus upon geminate recombination,[19,46,47] where the ligand re-

(46) Duddell, D. A.; Morris, R. J.; Richards, J. T. *J. Chem. Soc., Chem. Commun.* **1979**; 75.
(47) Alpert, B.; Mohsni, S. E.; Lindqvist, L.; Tfibel, F. *Chem. Phys. Lett.* **1979**, *64*, 11.
(48) Cornelius, P. A.; Hochstrasser, R. M.; Steel, A. W. *J. Mol. Biol.* **1983**, *163*, 119–128.
(49) Dlott, D. D.; Frauenfelder, H.; Langer, B.; Roder, H.; DiIorio, E. E. *Proc. Natl. Sci. U.S.A.* **1983**, *80*, 6239–43.
(50) Austin, R. H.; Beeson, K. W.; Eisenstein, L.; Frauenfelder, H.; Gunsalus, I. C. *Biochemistry* **1975**, *14*, 5355–5373. Eisenstein, L.; Frauenfelder, H.; In "Biological Events Probed by Ultrafast Laser Spectroscopy"; Alfano, R. R., Ed.; Academic Press: New York, 1982; pp 321–33.
(51) Szabo, A. *Proc. Natl. Acad. Sci. U.S.A.* **1978**, *75*, 2108–2111.
(52) Agmon, N.; Hopfield, J. J. *J. Chem. Phys.* **1983**, *79*, 2042.
(53) Morris, R. J.; Gibson, Q. H. *J. Biol. Chem.* **1982**, *725*, 4869–74.
(54) Brzowoski, A.; Derewenda, Z.; Dodson, E.; Dodson, G.; Crabowchi, M.; Liddington, R.; Skarginski, T.; Vallely, D. *Nature (London)* **1984**, *307*, 74.
(55) Szabo, A.; Perutz, M. F. *Biochemistry* **1976**, *15*, 4427. Perutz, M. F.; Kilmartin, J. D.; Nagai, K.; Szabo, A.; Simon, S. R.; *Biochemistry* **1976**, *15*, 378. Nagai, K.; Wilborn, G.; Dolphin, D.; Kitagawa, T. *Biochemistry* **1980**, *19*, 4755.
(56) Scheidt, W. R.; Brinegar, A. C.; Ferro, E. B.; Kirner, J. F. *J. Am. Chem. Soc.* **1977**, *99*, 7315.

binding is exclusively from a population of intraprotein ligands.

Geminate Recombination and Protein Structure. It has been observed that at both ambient[6,12,19,46-49] and cryogenic temperature,[49,50] photodissociated ligands have a finite probability of rebinding to the heme without having diffused into the surrounding solvent. This process is termed geminate recombination. At room temperature there appears to be two time scales associated with geminate recombination: a subnanosecond recombination and an ~100-ns recombination. The rate of the former is highly ligand dependent whereas the latter rate is relatively ligand independent. We have explored[13] a two-barrier model for the heme pocket to account for these two rates. These two barriers are shown in Figure 14. At the instant of photolysis, the Fe–ligand bond, Hb–X, is severed but there is an interval of time over which the ligand can rebind without having substantially diffused away from its original position. The deoxy photoproduct and the "frozen" ligand are designated as deoxy [Hb*·X] in Figure 14. Barrier I which modulates the rebinding at this phase (analogous to the innermost barrier of ref. 46 and 50) would be relatively free of diffusion-related parameters but would depend upon the configuration of the heme and relevant parts of the surrounding heme pocket. Transient picosecond absorption studies[48] and transient Raman at cryogenic temperatures[51] strongly suggest that this barrier is lowest for NO and highest for CO with O_2 being intermediate. If the ligand diffuses away from the heme into the surrounding protein, [Hb* + X], the subsequent rebinding rate for a fixed configuration is now primarily determined by a second barrier, labeled II, which originates from a diffusion-modulated process which is insensitive to the ligand and protein structure.

It has recently been pointed out that a correlation exists between the frequency of the Fe–His mode in deoxy Hb*(10 ns) and the yield of geminate recombination for both the faster and the slower processes.[13,32,33] This relationship was obtained by comparing, for two closely related photolyzed samples, both the frequency of the Fe–His mode and the yield of geminate recombinations averaged over either the first 10 ns subsequent to photolysis or the longer μs time averaged quantum yields of photolysis. Since the subpicosecond electronic relaxation associated with the photolysis appears[8] to be and is expected to be insensitive to protein structure it was assumed that for a given ligand, differences in the ligand-specific short time averaged yields of photolysis are due to protein-induced differences in the subnanosecond yield of geminate recombination. It is observed that for any pair of deoxy Hb*(10 ns)'s derived from a given hemoglobin but maintained under different solution conditions (i.e., pH, phosphate, etc.), the sample with the lower Fe–His frequency (i.e., more "T"-like) had the higher yield of photolysis. The relationship holds for both R-state comparisons as well as R–T comparisons. Modification of the distal heme pocket as in Hb (Zürich) does not alter this relationship.[41] A similar relationship was reported earlier involving the frequency of the oxidation state marker band at ~1355 cm^{-1}. This finding is not surprising given the inverse linear correlation between the frequencies of these two Raman-active modes.[16,17,27] On the basis of these relationships it was concluded[13] that the structural parameter modulating the frequency of the Fe–His mode (and the 1355-cm^{-1} mode) must also be modulating the height of barrier I and the depth of the ligated heme potential wall (A). An increase in the tilt of the histidine would destabilize the ligated heme because of the increased energy associated with making a planar geometry. The potential well for the ligated heme pocket (A in Figure 14) is therefore shallower for the more tilted geometry. To the extent that the transition state associated with barrier I resembles the planar ligated heme, it too is destabilized by forces favoring a tilt of the histidine. For slow-binding ligands such as CO, the transition state is thought to resemble the ligated heme more so than the deoxy heme;[51] consequently, for CO a decrease in the well depth of A would be closely matched by an increase in barrier I. In this case an increase in the histidine tilt might therefore have a relatively small effect on the spontaneous dissociation rate A → B) but instead decrease the rebinding from B or C to A. Fast-binding ligands such as O_2 and NO are expected to have transition states that primarily resemble the deoxy heme.[51]

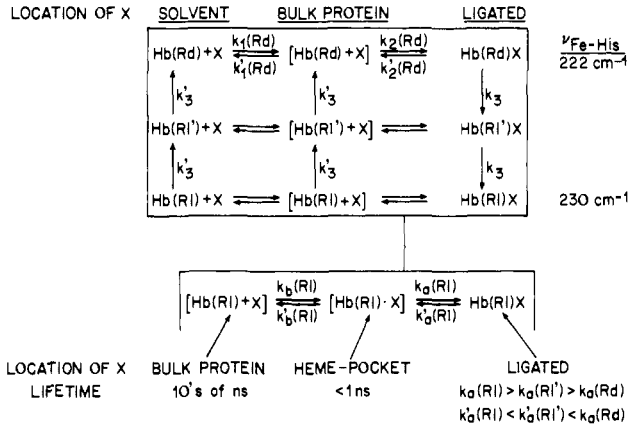

Figure 15. Scheme for understanding solution-dependent variation in the ligation properties within the R quaternary state based upon spectroscopically identifiable intermediates. Instead of Hb* and ligated Hb the various deoxy and ligated hemes are identified according to the tertiary structure: Hb(Rd), Hb(R*l*), and Hb(R*l*) refer to deoxy hemes imbedded in proteins having deoxy R, ligated R, and intermediate tertiary structures, respectively, while the corresponding ligated forms are designated by the same nomenclature but followed by an X. For example, Hb(Rd)X would be a ligated heme surrounded by the deoxy R tertiary structure. At the bottom of the figure is shown the breakdown of the processes that were lumped into the k_2 and k_2' steps within the box. The various k_2's for example refer to the overall geminate recombination associated with differing tertiary configurations. This process is broken down in the recombination derived from the bulk protein as well as from within the heme pocket. Tertiary-structure modulation of the geminate process occurs at level k_a and k_a' which are related to the proximal histidine controlled barrier I and well A of Figure 14. On the right side of the figure are shown the values of ν_{Fe-His} associated with Hb(Rd) and Hb(R*l*) derived from HbA. The larger the value of ν_{Fe-His} the greater is k_a and the smaller k_a'.

For these ligands the major effect of the tilt is expected to be the change in the well depth of A. Since for these ligands the transition state will be much less influenced, the histidine tilt induced effects, especially for the weakly bound O_2, will arise primarily from the change in the intrinsic rate of spontaneous dissociation (A → B).

Tertiary-Structure Relaxation and Reactivity: Kinetic Cooperativity. The results presented in this paper show that the time evolution of ν_{Fe-His} in photolyzed hemoglobins is solution dependent. At low pH this evolution is appreciable over the time scale for geminate recombination. Given the relationship between this frequency and ligand dynamics, there are significant implications associated with this fast pH-dependent relaxation. Both this work and earlier studies[13,31,32] have revealed two distinct tertiary states of the heme pocket for both the R and T quaternary structures. When the heme remains ligand bound over an interval of time that is long compared to the tertiary relaxation, then the predominant configuration of the heme pocket is characterized as the ligated tertiary structure, e.g., Hb(R*l*) or Hb(T*l*). For R-state HbA, this tertiary structure is associated with a frequency of ~230 cm^{-1} for ν_{Fe-His}, an absence of a distinct 345-cm^{-1} band, and an enhancement of the intensity of the Fe–His band relative to the ~300- and 360-cm^{-1} bands. Alternatively, when on the average the heme is ligand free for intervals of time that exceed the tertiary relaxation time, then the configuration of the heme pocket is characterized as the deoxy tertiary structure, e.g., Hb(Rd) or Hb(Td). This geometry is associated with a lower frequency (~222 cm^{-1} for Hb(Rd)) and lower intensity Fe–His band as well as a distinct 345-cm^{-1} band. Because the pH-dependent rate of tertiary relaxation in the R state scales with but is faster than the rate of the R to T transitions, we can discuss the tertiary structure of the R state in terms of quasiequilibrium between the ligated and deoxy tertiary structures. This quasiequilibrium is shown in Figure 15.

Prior to photolysis, the equilibrium favors the ligated R structure. Over the first few nanoseconds of photolysis the potential surface describing the ligand dynamics is still that of the

ligated R structure. For those heme pockets where the heme is no longer ligated, the equilibrium is shifted toward the deoxy R structure. The time evolution of Raman spectra reflects the associated change in structure about the heme. This change in structure is associated with a decreasing ν_{Fe-His}, hence (see Figure 14) the potential well A is becoming shallower by an amount δ and the height of barrier I is increasing by δ^* with $\delta > \delta^*$ by an amount that is ligand dependent. The results shown in Figure 5 indicate that k and probably k', the ligated to deoxy and the deoxy to ligated relaxation rates, respectively, are pH dependent. Consequently if we have two ligated heme pockets starting at Hb(R*l*) undergoing photolysis but at different pH's, then at some Δt later (where t is >10 ns) the potential surface for lower pH sample will have the higher barrier (I) and shallower well (A). Consequently, relative to the high-pH sample, the time-evolved configurations of heme pocket in the low-pH sample will favor the continued evolution of a ligand-free heme because the probability for recombination is lower. Thus, the low pH induced faster rate of relaxation should be associated with a lower yield of geminate recombination which further maintains the shift in equilibrium toward the deoxy R heme pocket geometry. Therefore, ligated R-state hemoglobins having the identical ligated heme pocket configuration (but presumably have differences elsewhere in the protein) will show differences in parameters of ligand reactivity such as the geminate yield, the quantum yield of photolysis, and the R-state macroscopic ligand off rates due to solution-induced differences in the rate of tertiary relaxation subsequent to either photoinduced or spontaneous ligand dissociation.

In Figure 6 it can be seen that for O_2HbA both geminate recombination and bimolecular recombination differ between pH 8.2 and pH 7 + IHP. Under these conditions we have observed that both ν_{Fe-His} for Hb(R*l*) and the yield of photolysis averaged over the first 10 ns are very nearly the same. Thus it appears very likely that the progressive pH-dependent divergence in the geminate and bimolecular yields is due to the pH-dependent difference in the quasiequilibrium between Hb(R*l*) and Hb(Rd).

Ligand-specific differences in the response of the geminate process to the pH-dependent changes in the rates of tertiary relaxation have not been studied. It is however, quite likely that a difference between O_2 and CO exists on the basis of the iron–ligand bond strength. The strong binding of CO makes it likely that once it rebinds the partially relaxed heme pocket is driven back to the end point ligated tertiary configuration. For O_2, spontaneous dissociation (A → B) of the destabilized religated species may be a dominant effect. Once the structure has relaxed from the ligated R structure, the probability that the geminately rebound ligand remains tightly bound to the iron for an interval sufficiently long to regain the ligated tertiary structure will be less for O_2 than for CO. Consequently, whereas O_2 may show pronounced changes in the geminate rebinding as a result of pH-induced changes in the tertiary relaxation, CO might not. Changes in the yield for CO are, however, expected in going to the pH + IHP extreme where the end point ligated R structure is statically modified (ν_{Fe-His} changes from 230 to 226 cm^{-1} for Hb*(10 ns)).

The generalized scheme to account for the kinetic basis of variations in ligand-binding properties within the R state is given in Figure 15. In the upper left-hand corner is the representation for the configuration of a deoxy R-state heme pocket—Hb(Rd). The ligand is initially in the solvent. Proceeding horizontally from left to right we follow the ligand from the solvent through the bulk protein and eventually to the heme. These steps are analogous to Frauenfelder's sequential scheme for binding in myoglobin.[50] It is assumed that the heme pocket does not begin to evolve until the ligand binds. Once the ligand binds, the heme pocket beings to evolve toward the ligated configuration Hb(R*l*) at a solution-dependent rate κ_3. As it evolves there is an off rate κ_2'(R*l*) and an on rate κ_2(R*l*) associated with each instantaneous configuration Hb(R*l'*). Since the lowest off rate and highest on rate are associated with the fully evolved ligated configuration, Hb(R*l*), the faster κ_3 is, the less likely is a dissociative event. Upon dissociation the system beings to evolve back toward Hb(Rd). If this solution-dependent rate, κ_3, is fast enough the deoxy heme "self-traps" in that the evolving pocket modifies the barrier (I) and the well (A) fast enough to make the geminate rebinding during the ~100-ns window less likely. Once the ligand is beyond the domain of geminate rebinding, the pocket will continue to evolve until a rebinding occurs from the solution-based population. At the bottom of the figure is a breakdown of the geminate process into the bulk protein derived and heme pocket derived populations which exposes the level at which protein control of ligation is exerted. This scheme clearly reveals that correlations between on rates and geminate recombination rates within a given quaternary structure are not straightforward. The on rate process starts with Hb(Rd) + X and presumably ends with either XHb(R*l*) or XHb(R*l'*) whereas the geminate process occurs from the other end and involves a much shorter segment of time. Consequently, on rates are expected to be more responsive to factors that change κ_3 and κ_3^1 than is geminate recombination. The geminate process is most affected when the solution conditions bring about a static change in structure of Hb(R*l*) such as occurs[13] when going from high pH to pH 6.2 + 3 mM IHP (ν_{Fe-His} goes from 230 to 226 cm^{-1} for photolyzed COHbA).

This scheme incorporates both sequential and parallel processes of the kind described by Frauenfelder[50] and Hopfield,[52] respectively. In contrast to Hb, Mb does not exhibit a spectroscopically distinguishable ligated and deoxy tertiary structure with respect to ν_{Fe-His}[16,32,57] and the 345-cm^{-1} mode.[57] Both the 10-ns transient species and cryogenically trapped photolyzed intermediates show little if any differences with respect to deoxy Mb.[57] Consequently, the parallel evolution of ligand and protein coordinate shown here for Hb is not expected to play a major role in the ligation dynamics of Mb.

Temperature Effects. The spectroscopic characterization of the tertiary structure for deoxy transients allows one to generate what is essentially an instantaneous picture of the heme environment in ligated as well as deoxy species. In an attempt to understand the structural basis for observed temperature dependencies of oxygen binding in different hemoglobins we have probed the tertiary structure of ligated hemoglobins as a function of temperature. At low temperatures (~2 °C) the spectra of the photolyzed transients at 10 ns is both very nearly ligand independent and characteristic of the tertiary structure of a ligated heme pocket. At higher temperatures there is marked divergence in the spectra between tight-binding and weaker-binding ligands. As seen in Figures 7, 8, and 9 an increase in temperature for these oxyhemoglobins results in spectra that are more deoxy-like on the basis of the shift in ν_{Fe-His} and the appearance of the 345-cm^{-1} peak. The effect of the O_2 concentration is also readily observed. A decrease in oxygen concentration exaggerates the deoxy-like features of the spectra at the high temperatures. The addition of CO reverses these spectral changes. It can be seen from Figures 7 and 8 that the temperature effect upon the spectra of the oxy derivatives is most prominent at low pH where the affinity is lowest. A comparison of Figures 8 and 9 reveals that at pH 9 the sea turtle (*Chelonia mydas*) hemoglobin is more responsive to increases in temperature than in human Hb. Sea turtle Hb's are low-affinity hemolgobins with low values of ν_{Fe-His} even at high pH (see Figure 11). These results and the discussion presented in this manuscript suggest that there are two possible contributions to this temperature effect. When a ligand undergoes spontaneous dissociation the tertiary structure starts to relax. It has been shown in this work that this relaxation is pH dependent. Temperature changes affect the pK_a's of various amino acids which in turn modify the relaxation rates of the tertiary structure. Thus for a given interval over which a ligand remains off the heme, the tertiary-structure relaxation will proceed at a temperature-dependent rate. The temperature also affects the diffusion of the dissociated ligand through the protein. As the temperature increases the more likely is the ligand to diffuse away from the heme after dissociation. The net effect is to increase the average interval

(57) Argade, P.; Scott, T. W.; Friedman, J. M.; Rousseau, D. L., unpublished results.

over which the ligand remains away from the iron. The longer this interval the greater the amount of relaxation which makes subsequent rebinding less likely. At high pH for HbA the tertiary relaxation subsequent to dissociation proceeds very slowly and as a result, the spectra reflecting the relaxation are not affected by temperature as much as in the low-pH samples. It can be seen from Figure 7 and 8 that whereas at high pH the high-temperature spectra show only a slight degree of relaxation toward a deoxy-type spectrum, the faster relaxing low-pH sample exhibits a high-temperature spectrum that resembles the R-state deoxy species also shown in the figure. For the sea turtle (Figure 9) the pronounced temperature effect at pH 9 is likely to be due to the lower probability for rebinding (based on the value of ν_{Fe-His}) which keeps the ligand for longer intervals of time compared to HbA at pH 9. From the earlier analysis in this work it follows that the extent of relaxation from the end point ligated spectrum also reflects the average barrier height (I) and well depth (A) associated with ligand. In terms of Figure 15, the temperature alters the steady-state populations of Hb(Rd), Hb(R*l*′), and Hb(R*l*) by affecting k_3', k_3, and k_b' for the reason described above. An increase in Hb(R*l*′) and Hb(Rd) at the expense of Hb(R*l*) indicates a decrease in the overall ligand-binding affinity within the R quaternary state because $k_a(Rl) > k_a(Rl) > k_a(Rd)$ and $k_a'(Rl) < k_a'(Rl') < k_a(Rd)$ as shown in Figure 15. When the pH heavily favors the formation of a tight-binding Hb(R*l*)X(k_a(R*l*) large and k_a'(R*l*) small) as in the case of oxy or carboxy HbA at pH 9, spontaneous dissociation is a low-probability event. Consequently the ligated heme pocket tends to remain locked into the Hb(R*l*) configuration over a wide range of temperature. At lower pH values the rate of spontaneous dissociation for oxy HbA increases with increases the susceptibility of the system to temperature-dependent changes in k_3, k_3', and k_b' by generating a larger population of [Hb(R*l*)·X]. Similarly, the low intrinsic affinity of R-state Hb (*Chelonia mydas*) even at pH 9 (k_a(R*l*) small, k_a'(R*l*) large) results in sizable and hence temperature-vulnerable population of [Hb(R*l*)·X]. It is possible that in such low-affinity hemoglobins a stabilization of the affinity against drastic temperature effects may be achieved by a slow pH insensitive tertiary relaxation rate as suggested in Figure 5 for *Caretta caretta*. The addition of tight-binding ligands such as CO to any of these systems decreases the temperature effects by diminishing the population of [Hb(R*l*)·X].

In the three cases shown in Figures 7, 8, and 9, the trend is a decrease in binding with an increase in temperature. Figure 10 depicts the reverse pattern for carboxy hemoglobin from the bluefin tuna. The spectra reveal a shift with decreasing temperature from the ligated R- to the ligated T-state tertiary structures. Similar but far less extensive shifts have also been observed[24] for some sea turtle hemoglobins at pH 7.0. These Raman results directly verify earlier claims[53] that the reverse temperature effect in tuna is a result of a temperature-dependent shift in the R–T equilibrium. Thus if at low temperature there is a sizable population of T-state hemoglobin which upon raising the temperature would exhibit the normal decrease in affinity for the reasons discussed above, then a shift in the population to the R state can compensate for or even override the usual temperature effect.

Conclusions

Two spectroscopically distinguishable tertiary structures are evident in the heme pocket of both the R- and T-state quaternary structures of Hb. Within each quaternary structure ligation induces changes in the environment of the heme that transforms the deoxy R- or T-state heme pocket (designated as Hb(Rd) or Hb(Td), respectively) to the ligated R- or T-state heme pocket (Hb(R*l*) or Hb(T*l*), respectively). The frequency of the iron–proximal histidine stretching mode (ν_{Fe-His}) associated with the electronically relaxed deoxy heme increases on going from Hb(Td) to Hb(T*l*) ≈ Hb(Rd) to Hb(R*l*). With respect to a deoxy heme only Hb(Td) represents an equilibrium species for HbA. By following the evolution of ν_{Fe-His} subsequent to photolyzing COHb(R*l*), it is demonstrated that Hb* is initially Hb(R*l*) but relaxes with a solution-dependent rate to Hb(Rd) prior to the R–T switch. The functional significance of this solution-dependent relaxation is indicated by virtue of the involvement of ν_{Fe-His}. Previous studies[13,32] have revealed a correlation between geminate recombination and the structural determinants of ν_{Fe-His}. These studies allow for the attributing of a distinct configuration coordinate diagram to be associated with each value of ν_{Fe-His}. The relaxation experiments indicate that the potential surface controlling ligand bonding can change on the time scale of geminate recombination. On the basis of these findings a model is described incorporating both sequential and parallel processes that can account for variations in ligand reactivity within a given quaternary state.

Acknowledgment. The authors gratefully acknowledge the following individuals for their contributions of blood samples: Prof. S. Simon (Hb(cat), Hb(swordfish), and Hb(A)), Prof. P. Lutz (sea turtle blood), Prof. Q. Gibson (Hb(tuna)), Prof. E. Bunn (Hb(Kempsey)), Prof. R. Noble (Hb(carp)), Dr. S. Ogawa (Hb(Kansas)), Dr. V. Macdonald (Hb(Zürich), Prof. D. Jackson (Hb(painted turtle), and Prof. W. Frair (Hb(wood turtle)). Prof. S. Simon generously assisted in sample preparation as well as sharing with me unpublished kinetic and CD measurements on a variety of hemoglobin samples. Professors P. Lutz and W. Frair helped in the often difficult task of drawing blood from live sea turtles and fresh-water turtles, respectively.

Note Added in Proof. We have recently concluded a series of picosecond experiments which show that for both R- and T-state carboxyhemoglobins, the low-frequency transient Raman spectra at ~30 ps subsequent to photolysis are basically the same as those at 10 ns.

Registry No. HbA, 9034-51-9; COHbA, 9072-24-6; Hb Kempsey, 37248-11-6; O_2HbA, 9062-91-3; COHb Kansas, 39320-10-0.